Available online at www.sciencedirect.com

ScienceDirect

Procedia CIRP 00 (2023) 000–000

www.elsevier.com/locate/procedia

19th CIRP Conference on Modeling of Machining Operations

Coupled Dynamic Simulator With Tri-Dexel Milling Module For Robotic Machining Operations

Valentin Dambly *[a], Édouard Rivière-Lorphèvre[b], Olivier Verlinden[a]

[a]*Department of Theoretical Mechanics, Dynamics and Vibrations, University of Mons (UMons), Place du Parc 20, Mons 7000, Belgium*
[b]*Department of Machine Design and Production Engineering, University of Mons (UMons), Place du Parc 20, Mons 7000, Belgium*

* Corresponding author. Tel.: +3265374325. *E-mail address:* valentin.dambly@umons.ac.be

Abstract

In robotic machining, important tool-tip deviations occur resulting from lower stiffness as compared to CNC machines. Hence, this paper aims to present a coupled simulator developed in C++ for offline simulation of machine dynamics while operating, ultimately to estimate tool deviation and machined surface. The dynamic simulator of machine is coupled with a dexel-based machining module computing the forces as well as the updated workpiece geometry. The forces are computed by considering interference between dexel network and triangle-mesh sweep volume with relative closest triangle algorithm. Experimental milling tests are carried out for verification of forces, deviations and hence geometry.

Keywords: Virtual machining; robotic machining; 5-axis milling; tri-dexels; machine-tool dynamics

1. Introduction

Even though robotic machining is a fast-growing technology in the field of mechanical manufacturing with its costs savings and ability to work with complex geometries and trajectories, this technology is confronted to troubling phenomena. Indeed the counterpart for its mobility is the lower stiffness than conventional machine tools with, as an order of magnitude, $1N/\mu m$ for robots against about $50N/\mu m$ for machine tools [1]. Consequently, machining hard materials, leads to inaccuracies due to cutting forces. To improve the accuracy of robotic machining operations, it has been shown that a significant part of the deviations, up to 80%, can be compensated offline based on reliable models of the operation [1].

Furthermore, in the context of Industry 4.0 and its digital twins concept, virtual manufacturing has grown to become essential for the offline prediction of instabilities and online monitoring of operation. With accurate enough modelling of machining operation, the cutting conditions can be optimised to place the operation in a stable region by avoiding phenomena such as chatter vibrations, which is a current problematic met in robotic machining. In the context of model-based trajectory compensation, it is essential to model the dynamical behaviour of such flexible structure as well as the cutter-workpiece engagement (CWE) and the resulting forces along the tool while operating complex trajectories.

The paper first presents the numerical approach for dynamical simulations of machining operations and their purpose in machining modelling in general. Afterwards, the coupled machining simulation principle is presented with further details on the CWE determination, covering the definition of the swept surface as well as the handling of multi-dexel networks, up to the modelling of the system dynamics. Initially, the novelty of the approach lies on the methods used to determine the intersection between the workpiece and the tool swept surface, but also in the coupling of a multibody model including tri-axial flexibility with a machining simulator. The coupled model simulator is compared in terms of forces and machined surfaces to data measured in robotic machining cell for linear trajectory. Eventually a 5-axis motion is simulated to illustrate the CWE determination capability.

2. State of the art

Obviously, the modelling approach has to be chosen depending on the goal of the simulation. From micro-mechanics to macro-mechanics levels, their purposes and benefits are strongly different [2]. In robotic machining, the main interest is the ability to predict the stability of the operation and the tool deviation. The simulation level of robotic machining lies then in macro-mechanics level where the focus is on estimating the machining forces.

There are many workpiece modelling approaches able to deal with complex tool motions. For a more global view of the operation and volume removed, where only the tool envelope is considered, the Constructive Solid Geometry enables excellent estimation of machined surface [2]. The quality and the stability of a machining operation strongly rely on the machine tool behaviour while subjected to cutting forces. Thus, for dynamical simulation, the modelling of cutting edges motion is required to determine the evolution of the forces at each step. In such cases, discrete modelling approaches, with especially voxels [3] and dexels [4], are preferred.

The dexel approach presents interesting characteristics in terms of memory consumption and interference computation, making this method widely used in dynamical simulation of machining operations [5]. During the simulation, the update of the dexel network implies to determine if extremities are located inside the volume swept by the edges. This geometry problem can be approach by considering the concept of oriented volume described by Denkena *et al.* [6] or with point-in-volume algorithms [7],[8].

There also exist several approaches for the modelling of machine tool dynamics. The modal parameters can be directly considered [9], [10]. However in the case of robots, due to their highly non-linear dynamics, multibody approach is considered for more general reproduction of their behaviour in the whole workspace [11]. Stavropoulos *et al.* proposed a dynamical simulator explicitly coupling machine dynamics models with commercial CAM software where the CAM software is used to get an estimation of the forces along the operation. This signal is applied as an external excitation on the multibody model to iteratively get an estimated deflection at the tool tip [12].

In the frame of this research, the focus is on the dynamic response of the system. Hence, the cutting forces as well as the machined surface are computed by a module communicating with the machine tool dynamical model at each time-step.

Nomenclature

CWE	Cutter-workpiece engagement
RCT	Relative Closest Triangle

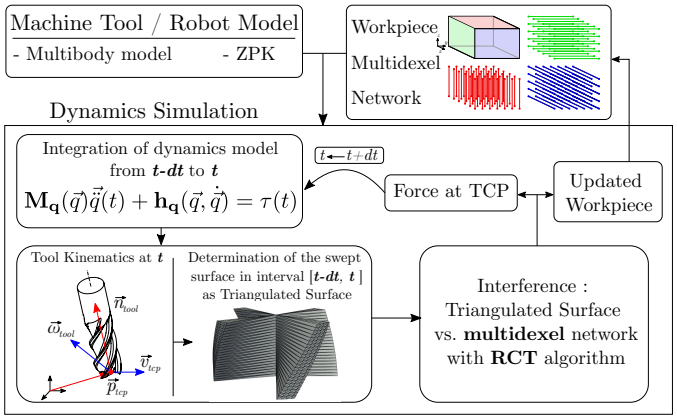

Fig. 1: Flow chart of the simulation process. The visualisation of tool cutting edge swept surface triangulated is carried out with VTK through Pyvista [15].

$d_{dex,i}$	Discretisation of dexel grid along i axis
$h_{k,j}$	Uncut chip thickness for slice k at tooth j
$\mathbf{K}_c$	The shear force coefficients $[MPa]$
$\mathbf{K}_e$	The edge force coefficients $[N/mm]$
dz	Height of the tool slice
dS	Elementary edge length of the tool slice
$\mathbf{R}_{i,j}$	Rotation matrix from frame i to j ($\in SO_3$)
$\mathbf{M_q}(\vec{q})$	Mass matrix of the system depending on $\vec{q}$
$\mathbf{h_q}(\vec{q},\dot{\vec{q}})$	Vector regrouping the Coriolis, gyroscopic and centrifugal forces
$\vec{\tau}(t)$	External forces applied on the system

3. Numerical Approach

The simulation of machining operations in this work lies on the determination of the cutter workpiece engagement, depending on the modelling approach of the workpiece, and the model of the machine tool. The workpiece is modelled with a discrete approach, namely a multi-dexel network. Following the convention in mechanistic approach [13], the solid mill is discretized in slices along its revolution axis. The simulation process requires the model of the workpiece as well as the dynamical model of the machine tool. In the specific case of this work, the machine tool is an industrial robot. The simulation consists in the integration in time of the dynamical equations of the model where the external applied forces at the tool tip are the machining forces computed with a machining module, updating the part as well [14]. The flow chart of the process is detailed in Figure 1.

3.1. Modelling of tool-workpiece interference

As introduced, the cutting is characterised by the cutter-workpiece engagement. The CWE is determined by the interference of the surface swept by the cutting edges and the network of dexels. The CWE is refreshed at each time step, which

enables to capture the effect of the robot vibrations on the shape of the cutting forces as well as in the resulting cut dexels. As illustrated in Figure 1, at each time step of the simulation, the kinematics of the TCP is known. As a result, the position and velocity of each point along the cutting edges can be computed from the velocity field of the tool body as long as this body is defined (as a rigid body or more sophisticated models). From the edges kinematics, known at times $t-dt$ and t, with dt the integration time step, intermediate positions are computed using Hermite Splines, creating a point cloud, which can be converted to a triangulated surface. Its illustration is given in Figure 2 for common tools with a flat-end mill and a ball-end mill. Since the swept surface ($\mathcal{S}$ for a single tooth in Fig. 2) is basically a set of triangles, the computation of intersection with dexels is direct. Several cases are possible when dealing with a dexel: it can be shortened, divided or removed. The first test is to check if nodes of the dexel are comprised in the volume enclosed within the swept surface. To check if a point is inside a volume or not, efficient methods have been proposed with PinMesh algorithm [7] and the relative closest triangle (RCT) [8]. Since the amount of vertices and triangles is rather low compared with the test cases in [7], the RCT algorithm is preferred with its forward preprocessing of the point cloud and low query time.

The common case is to have a node fulfilling the *inside volume* condition along with an intersection with a triangle $\in \mathcal{S}$, leading to the dexel being shortened. If no nodes are enclosed in the volume and two intersections are computed, the dexel is divided, creating an opening in the workpiece. Finally, if the two-ends fulfil the condition, the dexel must be removed.

As mentioned, the workpiece is modelled with dexels and it is well-known that the main drawbacks of every discrete modelling methods, including dexels, are the aliasing error and the management of the memory. The management of the memory covers the volume required to store the information as well as its handling in the simulation. The voxel method is a typical illustration the impact of such phenomena where the octree approach has been brought to strongly reduce their impact on the simulation performances [3]. The concept is to subdivide the model into a reduced number of subsets with a rougher resolution than the model resolution. With this approach, the subsets can be efficiently sorted in either likely

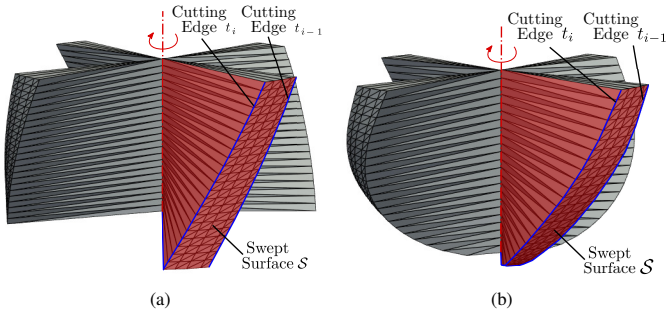

Fig. 2: Triangulated swept surface in the time interval $[t-dt, t]$ for 4 teeth tools : (a) Flat-end mill, (b) Ball-end mill.

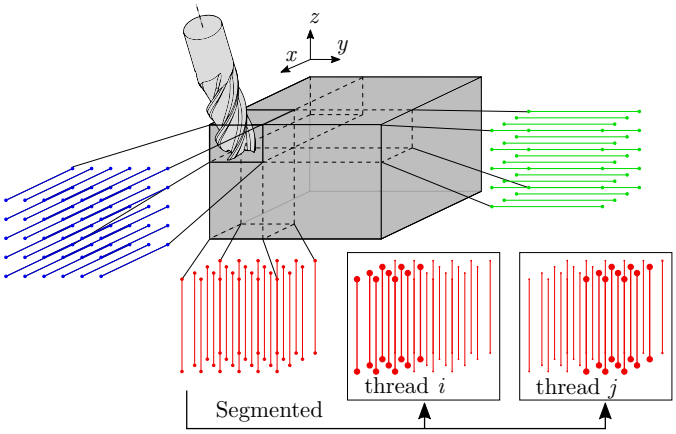

Fig. 3: Representation of the workpiece in multi-dexel network. Illustration of the segmentation of dexel network in subsets.

to collide with tool or no collision by using Boolean tests [10].

In Figure 3, where the workpiece is discretized in dexels, only the subsets interfering with the tool are shown and represent the ones actually checked for interference. In order to exploit computation capability, the intersection computation is parallelized by assigning a thread to each subset as explicitly shown for the dexel network along z direction.

3.2. Modelling of process dynamics

The industrial robot is modelled as a multibody system where its flexible behaviour is taken into account. The structural flexibility is modelled through equivalent beams and the articular one is modelled with the tri-axial flexibility approach for each articulation [11]. The general expression of the dynamical equations is given by:

$$\mathbf{M_q}(\vec{q})\,\ddot{\vec{q}}(t) + \mathbf{h_q}(\vec{q}, \dot{\vec{q}}) = \vec{\tau}(t) \tag{1}$$

where $\mathbf{M_q}(\vec{q})$ is the mass matrix, $\mathbf{h_q}(\vec{q}, \dot{\vec{q}})$ is the vector regrouping the Coriolis, gyroscopic and centrifugal forces and $\vec{\tau}(t)$ the vector of external forces applied on the system.

$$\vec{\tau} = \sum_{i=1}^{n_B} \left([\mathbf{J}_{S,i}]^T_{Base} \cdot \{\mathbf{R}_i\}_{Base} + [\mathbf{J}_{\omega,i}]^T_{Base} \cdot \{\mathbf{M}_{G,i}\}_{Base} \right) \tag{2}$$

where the subscript *Base* refers to the base frame, $[\mathbf{J}_{S,i}]_{Base}$ and $[\mathbf{J}_{\omega,i}]_{Base}$ are the translational and rotational Jacobian matrices of body i expressed in the base frame. According to the tri-axial flexibility approach, the flexibility is modelled by introducing unactuated degrees of freedom q_u in each of the principal direction x, y, z of the articulation and apply forces on bodies from both side of this articulation. The forces applied to body i are gathered in the resulting force $\{\mathbf{R}_i\}_{Base}$ and moment $\{\mathbf{M}_{G,i}\}_{Base}$. The action (a) - reaction (r) torques between body i and j are expressed:

$$\begin{aligned} \{\mathbf{M}_{G,i}\}_{Base} &= -\left(k_{q_u} q_u + d_{q_u} \dot{q}_u\right) \cdot \mathbf{R}_{Base,i} \cdot \vec{u}_{x,y,z} \quad \text{(a)}, \\ \{\mathbf{M}_{G,j}\}_{Base} &= \left(k_{q_u} q_u + d_{q_u} \dot{q}_u\right) \cdot \mathbf{R}_{Base,i} \cdot \vec{u}_{x,y,z} \quad \text{(r)} \end{aligned} \tag{3}$$

where k_{q_u} and d_{q_u} are the torsional stiffness and damping of the articulation respectively along $\vec{u}_{x,y,z}$, being the local unit vectors. The stiffness and damping coefficients have been identified by fitting the simulated frequency response functions from the multibody model with data from experimental modal analysis (EMA) according to the forward fitting method described by Huynh *et al.* [11], [16].

The machining forces are computed as the sum of the elementary contribution of each slice where this contribution $d\vec{F}$ is determined with the mechanistic approach [13] :

$$dF_i = \mathbf{K}_{i,c} \cdot h \cdot dz + \mathbf{K}_{i,e} \cdot dS \quad (4)$$

with $i = t, r, a$ being the tangential, radial and axial directions, h the chip thickness, dz the height of the slice and dS the edge length. The coefficients $\mathbf{K}_{i,c}$ and $\mathbf{K}_{i,e}$ represent shear contact pressure $[MPa]$ and the non-shearing flank line contact force $[N/mm]$ respectively. They must be identified experimentally by fitting the linearized force model. The key element to determine in Equation 4 is the chip thickness h, resulting from the evaluation of the CWE. The chip thickness is estimated by locally reconstituting the front of matter, at each step, with the dexel network and the tool kinematics using Hermite Splines [14]. The computed machining forces are applied to the system through $\{\mathbf{R}_{tool}\}_{Base}$ the resultant of applied forces on the tool body.

4. Results

The coupled simulator results are compared with forces and surface measurements for a pass in half immersion of a flat-end mill. This section is concluded with a 5-axis motion to illustrate the ability of the proposed approach to compute the CWE and workpiece determination for varying axial and radial depth of cut.

4.1. Experimental setup

The industrial robot used in the faculty robotic machining cell is a Stäubli TX200 with a teknomotor spindle. The cutting forces signals in the X, Y and Z directions were measured with a Kistler 9257B force sensor and recorded with a Kistler charge amplifier 5070A and the data acquisition system (DAQ) Kistler 5697A2 where the sampling frequency was set at 40 kHz. The machined surfaces point clouds have been measured with a Coordinate Measuring Machine Wenzel LH57 with a 1.5 *mm* diameter probe. Further mentioned x, y, z directions are defined as follows: the feed direction is along the y axis, the tool axis is aligned along the z direction and, consequently, the x is the privileged direction to observe radial deviations as illustrated in Figure 4.

4.2. Linear motion

The operation measured is a linear pass in half-immersion in a block of Al6060, as illustrated in Figure 4. The operation and simulation parameters are gathered in Table 1. The forces are gathered in Figure 7 and the gap between machined surfaces and targeted surfaces are presented in Figure 5.

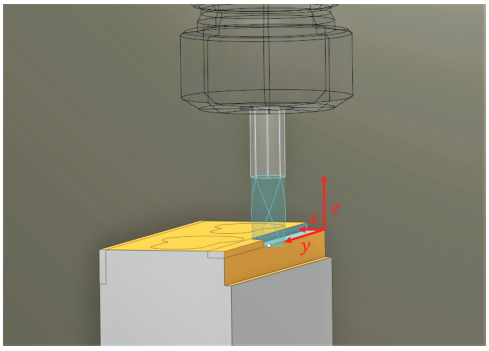

Fig. 4: Illustration in CAM software SprutCAM of the experimental pass with the chosen reference frame for measurements.

Table 1: Operation and simulation parameters. The shear force and edge coefficients have been previously identified and corroborate with literature [17].

Workpiece Material		Al6060
	Operation parameters	
Operation type		Half-immersion
Tool type		Cylindrical Flat-end
Tool material		Carbide
Diameter	$[mm]$	10
N° of edges (flutes)		2
Pitch	[°]	170-190
Helix angle	[°]	30
Rotation Speed	$[RPM]$	11250
Tooth feed	$[mm/tooth]$	0.13
Axial - Radial depth of cut	$[mm]$	2 - 5
	Simulation parameters	
Dexel Resolution $d_{dex,x}, d_{dex,y}, d_{dex,z}$	$[\mu m]$	100, 100, 50
Number of slices (tool)		16
Time steps dt	[s]	$1e-4$
$K_{t/r/a,c}$	$[MPa]$	733.5/346.5/127.9
$K_{t/r/a,e}$	$[N/mm]$	28.2/21.6/2.5

The forces along the global x, y, z directions are measured and compared with simulated forces. The RMS force in the $x-y$ plane is also given in Figure 7(a). The envelope shape of the forces for each of the global directions is given in Figures 7(b,c,d). Overall, the simulated RMS force in the $x-y$ matches the measurements, hence the mean level of excitation applied on the model is considered relevant. Some differences are however to mention in the x and z directions, where positive contributions are measured.

The measurement of the F_z signal underlines the limitation of the force model used for cylindrical tools since a positive contribution is measured. For stiff machine tool, the effect of the axial contribution is rather low [14]. However for flexible machines such as robots, the vibrations and deflections along the axial direction are strong and lead to higher forces than estimated. It shows that the model should be augmented by the effect of the front edge of the tool. Its effect should then be separately identified [18].

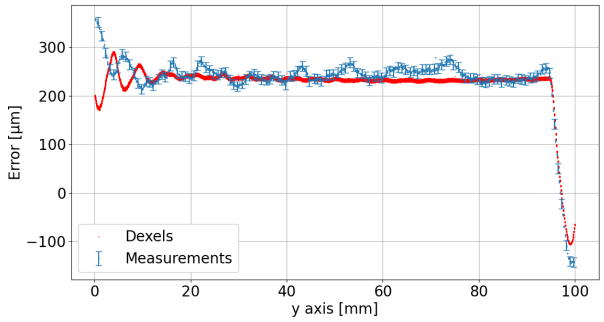

(a)

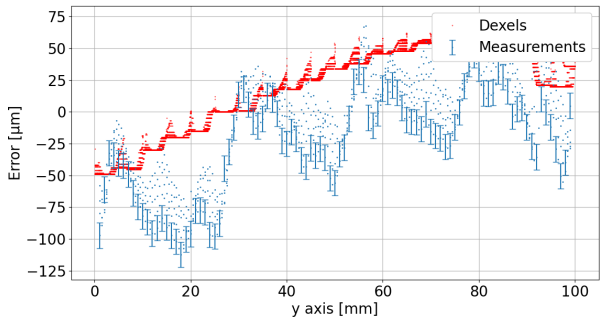

(b)

Fig. 5: Comparison between the point cloud measured with a Coordinate Measuring Machine of the surfaces resulting form the operation and the corresponding surfaces from the dexel network. (a) Error along the path (y direction) of the side surface : surface parallel to plan $y - z$. (b) Error along the path of the bottom surface : surface parallel to plan $x - y$.

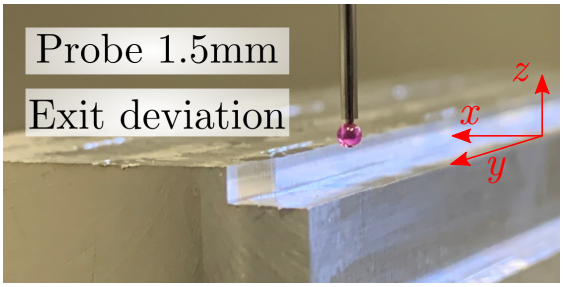

Fig. 6: Picture of the part where the tool exit, emphasizing the visible tool deviation.

The machined surfaces have been measured as a point cloud and compared to the dexel network in Figure 5. The simulated lateral surface presents the same characteristics as the measurements in terms of mean deflection while machining and the entrance-exit deviations with an amplitude of about 400μm. Where the exit of matter is properly estimated, the behaviour of the robot at the entrance reflects a lack of excitation in the dynamic simulation. The exit is shown in Figure 6 with the focus on the deviation. Meanwhile the deviation amplitude for the bottom surface measured is similar, it presents more variations with respect to the ideal plane as well as to the simulated resulting surface. This is a direct consequence of the excitation difference along the axial direction between the measured F_z and simulated one.

4.3. Five axis motion

In order to illustrate the capability of the cutting module to handle more complex tool motions, a 5-axis trajectory is considered where the tool follows an ellipse running alongside a cone. This motion gathers several challenges such as a varying radial and axial depth of cut with a changing orientation. This case is simulated with the aim of highlighting the robustness of the approach. The TCP path and tool orientation are illustrated in Figure 8a and the machined surface is shown in Figure 8b along with an illustration of the tool envelope evolution along the path in Figure 8c. Finally the machining forces are displayed in Figure 8d.

5. Conclusion

This paper presents a coupled simulator designed for the dynamical simulation of machine tools in operations. The research focuses on machining robots for the modelling the vibrations and deflections of these machines while subjected to machining forces. With the proposed approach for the modelling of the CWE, the dexel handling as well as its coupling with a multibody model of an industrial robot, the deviations of TCP are estimated properly in radial direction but improvements should be brought along the axial direction and in terms of model damping. It has been pointed out that the cutting force module itself reaches its limitation for the axial component and requires additional identification of the front edge effect. The approach considered for the determination of the CWE and dexel update was able to manage 5-axis tool motion cumulating challenges with varying depth of cut and tool orientation.

As stated in the Results section, a piece of the future works is the determination of machining forces model allowing a more realistic estimation of the axial force and the update of the multibody characteristics to meet a less stiff response. Alternatively, the estimation of the forces are accurate enough to estimate the deviations and vibrations induced by the robot in the radial direction, which makes it possible to propose alternative trajectories that compensate these deviations.

Acknowledgements

The authors would like to acknowledge the Belgian National Fund for Scientific Research (FNRS-FRS) for the grant allocated to V. Dambly.

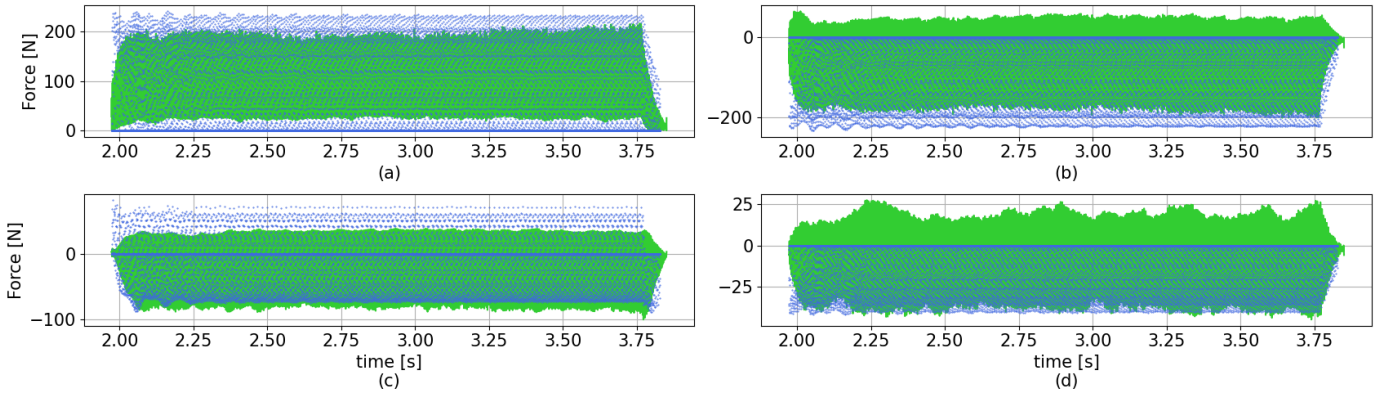

Fig. 7: Comparison of the machining forces between measured and simulated forces (blue: simulated; green: measured) for the linear trajectory with the parameters given in Table 1. (a) RMS Force in the $x-y$ plane (b) F_x (c) F_y (d) F_z.

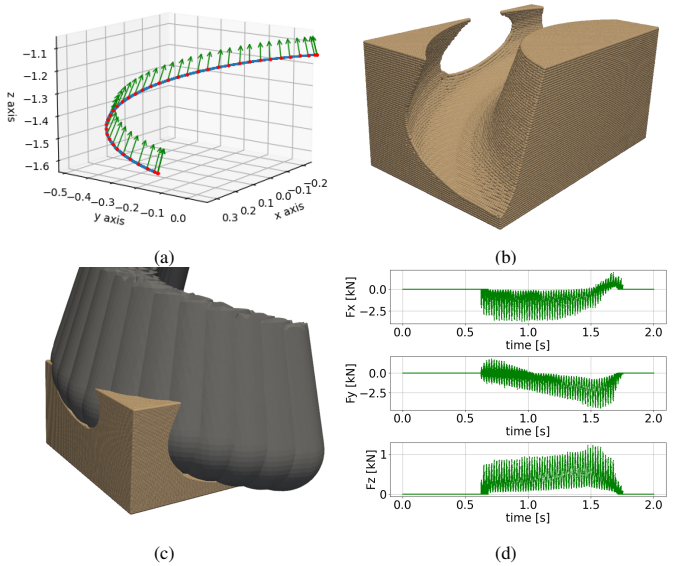

Fig. 8: Illustration of a machining operation with a 5 axis tool motion and a ball-end mill. (a) Tool trajectory; (b) Resulting workpiece; (c) Resulting workpiece with tool envelope; (d) Cutting forces (F_x,F_y,F_z).

References

[1] A. Verl, A. Valente, S. Melkote, C. Brecher, E. Ozturk, T. Tunc, Robots in machining, CIRP Annals (2019) 799–822.

[2] Y. Altintas, P. Kersting, D. Biermann, E. Budak, B. Denkena, I. Lazoglu, Virtual process systems for part machining operations, CIRP Annals - Manufacturing Technology 63 (12 2014).

[3] J. Joy, H.-Y. Feng, Frame-sliced voxel representation: An accurate and memory-efficient modeling method for workpiece geometry in machining simulation, Computer-Aided Design 88 (04 2017).

[4] B. Denkena, O. Pape, A. Kroedel, V. Böß, L. Ellersiek, A. Muecke, Process design for 5-axis ball end milling using a real-time capable dynamic material removal simulation, Production Engineering 15 (11 2020).

[5] M. Inui, M. Kobayashi, N. Umezu, Cutter engagement feature extraction using triple-dexel representation workpiece model and gpu parallel processing function, Computer-Aided Design and Applications 16 (2019) 89–102.

[6] B. Denkena, A. Kroedel, O. Pape, A. Muecke, L. Ellersiek, Identification of rake and flank face engagement parameters using a dexel-based material removal simulation with an oriented sweep volume, CIRP Journal of Manufacturing Science and Technology 35 (2021) 146–157.

[7] S. V. Magalhães, M. V. Andrade, W. R. Franklin, W. Li, PinMesh—fast and exact 3d point location queries using a uniform grid, Computers & Graphics 58 (2016) 1–11, Shape Modeling International 2016.

[8] J. Liu, Y. Chen, J. M. Maisog, G. Luta, A new point containment test algorithm based on preprocessing and determining triangles, Computer-Aided Design 42 (12) (2010) 1143–1150.

[9] H. N. Huynh, E. Rivière-Lorphèvre, F. Ducobu, A. Ozcan, O. Verlinden, Dystamill: a framework dedicated to the dynamic simulation of milling operations for stability assessment, The International Journal of Advanced Manufacturing Technology 98 (5) (2018) 2109–2126.

[10] B. W. Peukert, A. Archenti, A modular node-based modeling platform for the simulation of machining processes, euspen's 21st International Conference & Exhibition, Copenhagen (2021) 351–354.

[11] H. N. Huynh, H. Assadi, V. Dambly, E. Rivière-Lorphèvre, O. Verlinden, Direct method for updating flexible multibody systems applied to a milling robot, Robotics and Computer-Integrated Manufacturing 68 (04 2021).

[12] P. Stavropoulos, C. Gerontas, H. Bikas, T. Souflas, Multi-body dynamic simulation of a machining robot driven by cam, Procedia CIRP 107 (2022) 764–769, leading manufacturing systems transformation – Proceedings of the 55th CIRP Conference on Manufacturing Systems 2022.

[13] Y. Altintas, S. Engin, Generalized modeling of mechanics and dynamics of milling cutters, Cirp Annals-manufacturing Technology - CIRP ANNMANUF TECHNOL 50 (2001) 25–30.

[14] V. Dambly, Édouard Rivière-Lorphèvre, O. Verlinden, Tri-dexel based cutter-workpiece engagement determination for robotic machining simulator, Procedia CIRP 107 (2022) 1059–1064, Proceedings of the 55th CIRP Conference on Manufacturing Systems 2022.

[15] C. B. Sullivan, A. Kaszynski, PyVista: 3D plotting and mesh analysis through a streamlined interface for the Visualization Toolkit (VTK), Journal of Open Source Software 4 (37) (2019) 1450.

[16] H. Hoai Nam, Robotic machining: Development and validation of a numerical model of robotic milling to optimise the cutting parameters, Ph.D. thesis, University of Mons (09 2019). doi:10.13140/RG.2.2.32268.46726.

[17] M. Tsai, S. Chang, J. Hung, C. Wang, Investigation of milling cutting forces and cutting coefficient for aluminum 6060-t6, Computers & Electrical Engineering 51 (2016) 320–330.

[18] S. Bissey-Breton, Développement d'un modèle d'efforts de coupe applicable à des familles d'outils: cas du fraisage des aciers traités thermiquement, PhD Thesis (2005).